Overpressure prediction from PS seismic data

Robert J. Ferguson, Daniel Ebrom*

ABSTRACT

Mode converted shear waves have been shown to allow overpressure prediction in media where primary wave acquisition is inhibited by gas and fluid effects. This method proceeds through analysis of converted-wave moveout, and a long standing relationship between differential stress and changes in primary-wave velocity is modified in this prediction. Though empirical evidence from laboratory experiments and field experiments supports the stress / shear wave velocity relationship, a theoretical justification has been developed. In this paper, the original relationship is modified formally, and the overall procedure is outlined.

INTRODUCTION

Overpressure is a problem of which drilling safety requires that anomalous pressure cells and pressure gradients across faults, for example, can be mapped prior to drilling, (Snijder et al., 2002). For fixed depth, Eaton (1969) relates formation pressure gradient versus interval travel time The ratio of normally-pressured traveltime, Δt_n, and observed traveltime, Δt_0, are used to estimate the overburden stress gradient P/D according to

$$\frac{P}{D} = \frac{S}{D} - \left(\frac{S}{D} - \frac{P}{D_n}\right)\left(\frac{\Delta t_n}{\Delta t_0}\right)^E, \tag{1}$$

where S/D is the overburden stress gradient, and P/D_n is the normal pore pressure gradient. The exponent E is an empirical term determined from sonic transit-time logs obtained from a formation where it is normally pressured and from where it is overpressured, (Eaton, 1972). Eaton (1975) also relates formation pressure gradient to P- interval velocity. With the simple recognition that $\Delta t = \Delta z/\alpha$, where α is P-wave interval velocity, Eaton (1975) provides a revised pore-pressure prediction

$$\frac{P}{D} = \frac{S}{D} - \left(\frac{S}{D} - \frac{P}{D_n}\right)\left(\frac{\alpha_0}{\alpha_n}\right)^E, \tag{2}$$

where α_0 is the observed P-wave velocity, and α_n is the normally-pressured velocity. Ebrom et al. (2002) demonstrate that S-waves and C-waves are more sensitive to pressure gradients than P-waves. From their numerical experiment, Figure 1 shows that the percent change in P-wave stacking velocity is smaller than the change in S-wave and C-wave stacking velocities. For example, in this figure, for a shale zone overpressured 4000 psi above hydrostatic pressure for 3000 m depth, percent change in P-wave velocity is -2.5 where the changes are -3 and -3.5 for S-waves and C-wave respectively. Ebrom et al. (2003) adapt Eaton (1975) for S-waves for use in pore-pressure prediction. They verify experimentally good agreement between the Eaton (1975) equation (2) modified for S-wave interval velocity. They calculate a pressure curve for depth in an unknown basin and they

*StatoilHydro

compare this curve with the actual pressure curve encountered during drilling. Here, because surface mud weight is varied during drilling to prevent blowouts due to overpressure (and to prevent formation invasion when underpressure is encountered), it is a good proxy for the true pressure. As can be seen in the comparison of calculated and true curves, good agreement is obtained for this basin.

Kumar (2008) shows that, where gas clouds exist in the subsurface, PS-waves provide not only a better image, but the resulting stacking velocities are much more reliable. As Figure 3a demonstrates, pure P-wave recordings are impacted through bulk modulus on high gas content. Reflection events are discontinuous, and interpreted velocities vary strongly (3b) and are thought to be unreliable. Figure 3c shows a PS-wave section for the same traverse. Reflection events are more continuous, and the interpreted PS stacking velocities (Tessmer and Behle, 1988) vary more slowly and are thought to be more reliable for this reason.

Though the procedure is in use in industry, no formal justification for pressure prediction using PS-stacking velocity has been presented. In this paper, then, we present a theory to justify this usage. We begin with the basic P-wave based methods for interval velocity (Eaton, 1969, 1975), and we invoke the assumption of a laterally invariant ratio of S-wave and P-wave velocity to justify a pressure / S-wave velocity relationship. We convert these equations from interval velocity to stacking velocity using a simple argument, and we compute the product of the two results. This product allows us to replace products of P- and S-stacking velocities with PS-stacking velocity and provides the desired relationship. The resulting PS equation is very useful.

THEORY

Although they provide no formal justification, Ebrom et al. (2003) adapt equation 2 for use with S-wave interval velocity. Implicitly, they assume that the ratios $\alpha_n = \gamma_n \beta_n$ and $\alpha_0 = \gamma_0 \beta_0$ are constant for the formation, where β_n and β_0 are normally pressured S-wave velocity observed S-wave velocity respectively. Using this assumption, the ratio $\left(\frac{\alpha_0}{\alpha_n}\right)^E$ in equation 2 becomes

$$\left(\frac{\alpha_0}{\alpha_n}\right)^E = \left(a\,\frac{\beta_0}{\beta_n}\right)^E = \left(\frac{\beta_0}{\beta_n}\right)^{E+\varepsilon} = \left(\frac{\beta_0}{\beta_n}\right)^{E_\beta}, \tag{3}$$

where $a = \gamma_0/\gamma_n$, and E_β is an empirical constant to be determined from S-wave sonic logs. Based on S-wave interval velocity, then, equation 2 is given by

$$\frac{P}{D} = \frac{S}{D} - \left(\frac{S}{D} - \frac{P}{D_n}\right)\left(\frac{\beta_0}{\beta_n}\right)^{E_\beta}. \tag{4}$$

For simplicity, Ebrom et al. (2003) write equations 2 and 4 in terms of effective pressures

$$\sigma_{eff,n} = \frac{S}{D} - \frac{P}{D_n}, \tag{5}$$

and

$$\sigma_{eff,0} = \frac{S}{D} - \frac{P}{D}, \tag{6}$$

so that

$$\frac{\sigma_{eff,0}}{\sigma_{eff,n}} = \left(\frac{\alpha_0}{\alpha_n}\right)^{E} = \left(\frac{\beta_0}{\beta_n}\right)^{E_\beta} . \tag{7}$$

Ebrom et al. (2003), for an unknown region, determine a value of $E_\beta = 2$ based on their comparison using surface mud weights and S-wave sonic logs.

Though they do not provide an example, Ebrom et al. (2003) speculate that, in the absence of S-wave sonic logs, an alternative pressure-velocity relationship may be had based on PS-wave stacking velocity (Figure 2). Kumar et al. (2006) demonstrate the use of PS stacking velocity for offshore Trinidad & Tobago. Using stacking velocities for P-waves and S-waves (Dix (1955), and Appendix A, equations 34 and 35 respectively), equation 7 for a single depth becomes

$$\frac{\sigma_{eff,0}}{\sigma_{eff,n}} = \left(\frac{\tilde{v}_0^{\alpha}}{\tilde{v}_n^{\alpha}}\right)^{\tilde{E}} = \left(\frac{\tilde{v}_0^{\beta}}{\tilde{v}_n^{\beta}}\right)^{\tilde{E}_\beta} , \tag{8}$$

where $\tilde{E}$ and $\tilde{E}_\beta$ are new coefficients that correspond to P-wave and S-wave stacking velocities respectively. Though S-wave velocity is a rare measurement, PS-stacking velocity is readily available from PS-seismic analysis. To derive a pressure equation for PS-waves, write

$$\frac{\tilde{v}_{obs}^{\alpha}}{\tilde{v}_n^{\alpha}} = \left(\frac{\sigma_{obs}}{\sigma_n}\right)^{\frac{1}{E}} \tag{9}$$

and

$$\frac{\tilde{v}_{obs}^{\beta}}{\tilde{v}_n^{\beta}} = \left(\frac{\sigma_{obs}}{\sigma_n}\right)^{\frac{1}{E_\beta}} \tag{10}$$

and compute their product

$$\frac{\tilde{v}_{obs}^{\alpha}\,\tilde{v}_{obs}^{\beta}}{\tilde{v}_n^{\alpha}\,\tilde{v}_n^{\beta}} = \left(\frac{\sigma_{obs}}{\sigma_n}\right)^{\frac{1}{E}+\frac{1}{E_\beta}} . \tag{11}$$

Then, from Tessmer and Behle (1988) (Appendix A, equation 37), $\left(\tilde{v}^{\alpha\,\beta}\right)^2 = \tilde{v}^{\alpha}\,\tilde{v}^{\beta}$ and equation 11 becomes

$$\frac{\tilde{v}_{obs}^{\alpha\,\beta}}{\tilde{v}_n^{\alpha\,\beta}} = \left(\frac{\sigma_{obs}}{\sigma_n}\right)^{\frac{1}{2}\left(\frac{1}{E}+\frac{1}{E_\beta}\right)} . \tag{12}$$

The root of equation 12 gives the desired relationship between pressure gradient and PS-stacking velocity according to

$$\frac{\sigma_{obs}}{\sigma_n} = \left(\frac{\tilde{v}_{obs}^{\alpha\,\beta}}{\tilde{v}_n^{\alpha\,\beta}}\right)^{E_{\alpha\,\beta}} , \tag{13}$$

where $E_{\alpha\,\beta} = 2\,\frac{E_\alpha E_\beta}{E_\alpha + E_\beta}$ is a new coefficient for PS-waves.

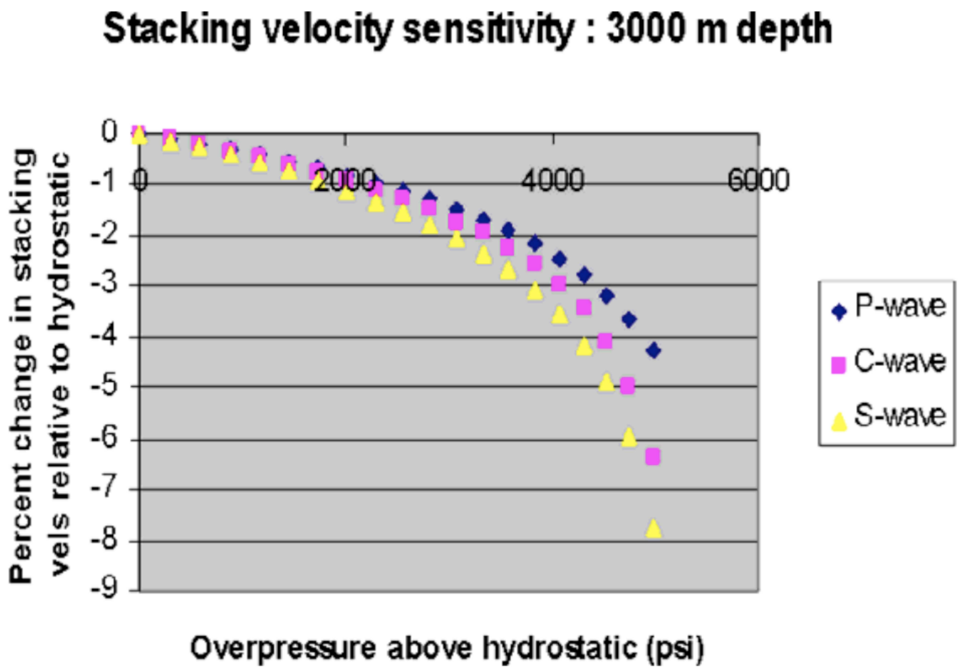

FIG. 1. Plot of % change in stacking velocity versus overpressure. For 3000m depth in this numerical experiment, S-waves and C-waves are more sensitive than P-waves. From Ebrom et al. (2002).

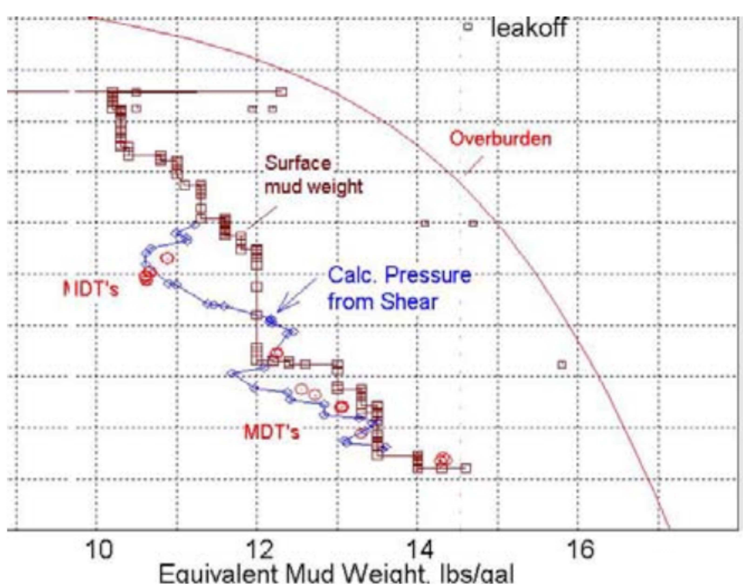

FIG. 2. Predicted pressure compared to pressure encountered during drilling. The predicted pressure is based on S-wave interval velocity obtained from dipole sonic logs. Note, the depth axis is omitted for proprietary reasons. From Ebrom et al. (2003).

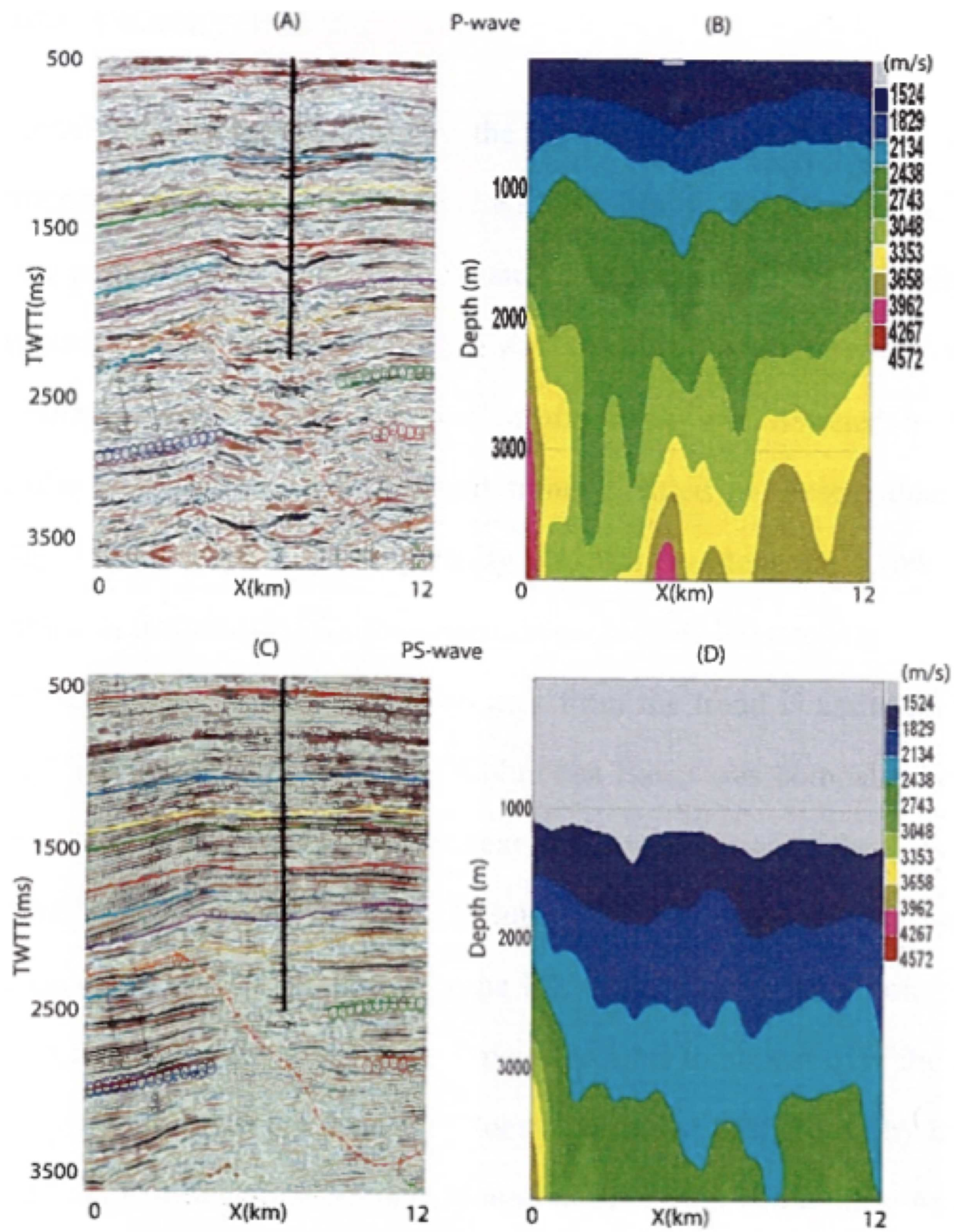

FIG. 3. Comparison of P-wave and PS-wave data. a) P-wave stacked section showing ambiguous reflectors due to a gas cloud. b) Corresponding P-stacking velocity. c) PS-wave stacked section showing continuous reflectors. d) Corresponding PS-stacking velocity. From Kumar (2008).

CONCLUSIONS

The method of Ebrom et al. (2003) that relates differential stresses due to anomalous pore pressure and converted-wave velocity is described analytically. The relationship between pure P-wave modes, S-modes, and the PS-modes is explored in the context of PS-wave velocity analysis. The PS velocity, rather than being inverted and analyzed as separate modes, is examined as it is, and pore pressure predictions are made. This approach has advantages in basins where overpressure hazards exist, and where gas and fluid effects preclude analysis using P-waves alone. Systematically, this approach is attractive because no specialized software needs to be developed for PS-wave velocity analysis or pore pressure prediction. PS moveout velocity is simply interpreted as is, and only the associated coefficient range differs from the P-wave range.

ACKNOWLEDGEMENTS

The authors wish to thank BP America, the sponsors of EDGER at the University of Texas at Austin, and the sponsors of CREWES for their support of this work.

APPENDIX A

This appendix follows closely the paper of (Tessmer and Behle, 1988) but, for clarity, we fill in a number of missing steps in that derivation. In general, reflection traveltimes T are hyperboloid functions of offset X

$$T_m^2 = a_m + b_m X_m^2 + c_m X_m^4 \cdots . \tag{14}$$

where, for the n_{th} interface, T_m is the reflection traveltime, X_m is the source-receiver offset, and $+$ve powers of X_m ensure $+$ve travel times. For simplicity, assume the relationship is hyperbolic

$$T_m = \sqrt{a_m + b_m X_m^2} \tag{15}$$

Estimate a_m and b_m to unravel z_m (thickness of n_{th} layer) and α_m and β_m — P- and S-velocity of the n_{th} layer respectively. Determination of a_m is easy, set $X_m = 0$ to get

$$T_{0,m}^2 = a_m \tag{16}$$

where $T_{0,m}$ is the zero-offset travel time for the m^{th} reflection. This leaves b_m in units of slowness squared $(s/m)^2$

$$b_m = \frac{T_m^2 - T_{0,m}^2}{X_m^2}. \tag{17}$$

The traveltime from the source to the n_{th} layer is the sum of the P-wave travel times through each layer

$$P_m = \left[P_1 + P_2 + \cdots + \frac{z_m}{\alpha_m \cos\theta_m} \right] = \sum_{j=1}^{m} \frac{z_j}{\alpha_j \cos\theta_j} \tag{18}$$

where z_j and θ_j are thickness and angle of refraction through the j^{th} layer respectively, and α_j is the corresponding P-wave velocity. The traveltime from the n_{th} layer to a receiver is the sum of the S-wave travel times through each layer

$$S_m = \left[S_1 + S_2 + \cdots + \frac{z_m}{\beta_m \cos\phi_m} \right] = \sum_{j=1}^{m} \frac{z_j}{\beta_j \cos\phi_j} \tag{19}$$

where ϕ_j is the refraction angle through the j^{th} layer, and β_j is the corresponding S-wave velocity.

The total traveltime T_m for a converted wave reflection from the m^{th} layer is the sum of the P-wave and S-wave traveltimes

$$T_m = P_m + S_m \tag{20}$$

or

$$T_m = \sum_{j=1}^{m} z_j \left[\frac{1}{\alpha_j \cos\theta_j} + \frac{1}{\beta_j \cos\phi_j} \right] \tag{21}$$

For general angle ψ and general velocity v, $\cos\psi = \sqrt{1 - \sin^2\psi}$, and from Snell's Law $\sin^2\psi = (vp)^2$ where p is ray parameter.

T_m, therefore, becomes

$$T_m = \sum_{j=1}^{m} z_j \left[\frac{1}{\alpha_j \sqrt{1 - (\alpha_j\, p)^2}} + \frac{1}{\beta_j \sqrt{1 - (\beta_j\, p)^2}} \right]. \tag{22}$$

On the P-wave side, the lateral distance x_j travelled through layer j is:

$$x_j = z_j \tan\theta_j = z_j \frac{\sin\theta_j}{\cos\theta_j} = \frac{\alpha_j z_j p}{\sqrt{1 - (\alpha_j p)^2}} \tag{23}$$

and a similar relationship will hold for the S-wave side.

For the m^{th} layer, then, total distance X_m is the sum of distances from the P-wave side and the S-wave side

$$X_m = p \sum_{k=1}^{m} z_k \left[\frac{\alpha_k}{\sqrt{1 - (\alpha_k p)^2}} + \frac{\beta_k}{\sqrt{1 - (\beta_k p)^2}} \right]. \tag{24}$$

To eliminate dependence on p, use the series for $[1 + u]^{-\frac{1}{2}}$

$$\frac{1}{\sqrt{1 - (\alpha p)^2}} \approx 1 + \frac{1}{2} (\alpha p)^2 . \tag{25}$$

As shown in Figure 4, only for $p = 0$ is the approximation exact, and T_m becomes

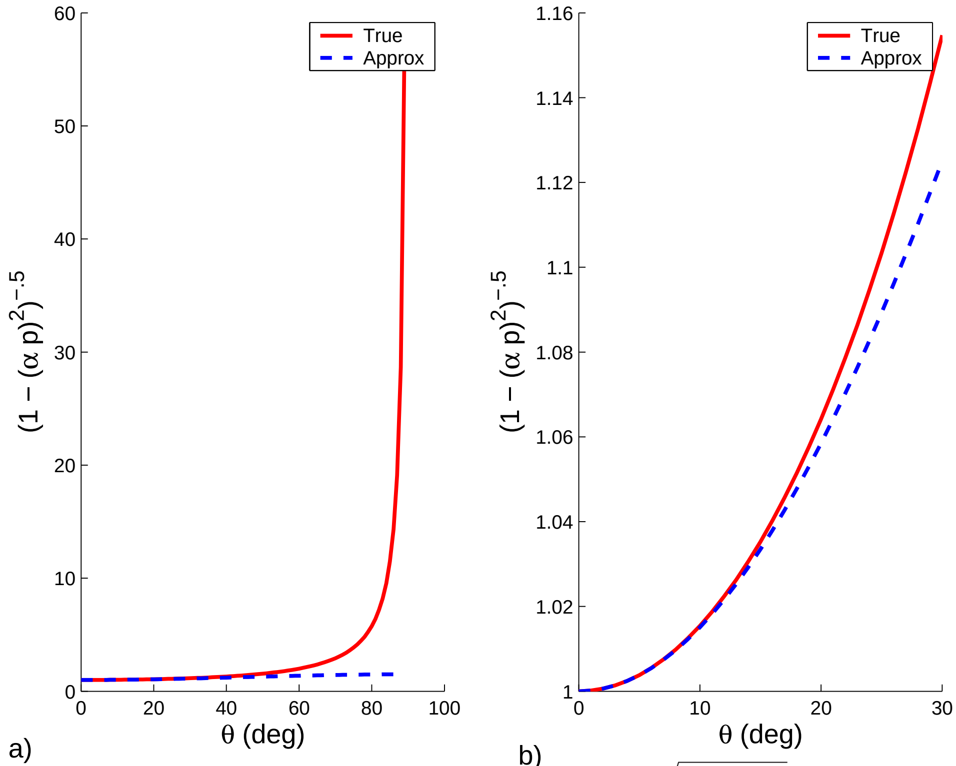

FIG. 4. Approximate vs. exact curve for $1/\sqrt{1-(\alpha p)^2}$ a). b) Zoom of a)

$$T_m \approx \sum_{j=1}^{m} z_j \left\{ \frac{1}{\alpha_j} \left[1 + \frac{1}{2} \left(\alpha_j\, p\right)^2 \right] + \frac{1}{\beta_j} \left[1 + \frac{1}{2} \left(\beta_j\, p\right)^2 \right] \right\}. \tag{26}$$

Using zero-offset time $T_{0;m} = \sum_{j=1}^{m} z_j \left[\frac{1}{\alpha_j} + \frac{1}{\beta_j} \right]$, T_m becomes

$$T_m \approx T_{0;m} + \frac{p^2}{2} \sum_{j=1}^{m} z_j \left[\alpha_j + \beta_j \right]. \tag{27}$$

Similarly, X_m becomes

$$\begin{aligned} X_m &= p \sum_{k=1}^{m} z_k \left\{ \alpha_k \left[1 + \frac{1}{2} \left(\alpha_k p\right)^2 \right] + \beta_k \left[1 + \frac{1}{2} \left(\beta_k p\right)^2 \right] \right\} \\ &= p \sum_{k=1}^{m} z_k \left[\alpha_k + \beta_k \right] + \frac{p^2}{2} \sum_{k=1}^{m} z_k \left[\alpha_k^3 + \beta_k^3 \right]. \end{aligned} \tag{28}$$

To find b_m, we need T_m^2 and X_m^2, but we're only keeping powers of p^2, so T_m^2 and X_m^2 become:

$$T_m^2 \sim T_{0;m}^2 + T_{0;m}\, p^2 \sum_{j=1}^{m} z_j \left[\alpha_j + \beta_j \right] \tag{29}$$

and,

$$X_m^2 \sim p^2 \left(\sum_{k=1}^{m} z_k \left[\alpha_k + \beta_k \right] \right)^2 \tag{30}$$

Using T_m^2 and X_m^2 above, b_m becomes

$$b_m = T_{0;m}\left(\sum_{k=1}^{m} z_k\left[\alpha_k+\beta_k\right]\right)^{-1} = \frac{\sum_{k=1}^{m} z_k\left[\frac{1}{\alpha_k}+\frac{1}{\beta_k}\right]}{\sum_{k=1}^{m} z_k\left[\alpha_k+\beta_k\right]} = \frac{\sum_{k=1}^{m}\left[\frac{1}{\alpha_k}+\frac{1}{\beta_k}\right]}{\sum_{k=1}^{m}\left[\alpha_k+\beta_k\right]}, \tag{31}$$

where we have used

$$T_{0;m} = \sum_{k=1}^{m} z_k\left[\frac{1}{\alpha_k}+\frac{1}{\beta_k}\right]. \tag{32}$$

For each reflector m, b_m is a measurable quantity - it is simply the second coefficient in a hyperbola fit to the m^{th} reflection event. Traveltime $T_{0;m}$ is also measurable - it is the projection to zero-offset of the n^{th} reflection event.

Define the *stacking* velocity for PS-waves, then, as

$$\left(\tilde{v}_m^{\alpha\beta}\right)^2 = \frac{1}{b_k} = \frac{\sum_{k=1}^{m}\alpha_k\left[1+\frac{\beta_k}{\alpha_k}\right]}{\sum_{k=1}^{m}\frac{1}{\alpha_k}\left[1+\frac{\alpha_k}{\beta_k}\right]}. \tag{33}$$

Assume now that $\frac{\beta_k}{\alpha_k}=\gamma$ is constant for all k, then $\gamma=\frac{\beta_k}{\alpha_k}=\frac{\beta}{\alpha}=\frac{\tilde{v}_m^{\beta}}{\tilde{v}_m^{\alpha}}$ where

$$\tilde{v}_m^{\alpha} = \sqrt{\frac{\sum_{k=1}^{m}\alpha_k}{\sum_{k=1}^{m}\frac{1}{\alpha_k}}}, \tag{34}$$

and

$$\tilde{v}_m^{\beta} = \sqrt{\frac{\sum_{k=1}^{m}\beta_k}{\sum_{k=1}^{m}\frac{1}{\beta_k}}}, \tag{35}$$

are stacking velocities for P-waves and S-waves respectively, and write equation 33 in terms of γ

$$\left(\tilde{v}_m^{\alpha\beta}\right)^2 = \frac{1+\gamma}{1+\frac{1}{\gamma}}\frac{\sum_{k=1}^{m}\alpha_k}{\sum_{k=1}^{m}\frac{1}{\alpha_k}} = \gamma\,\frac{\sum_{k=1}^{m}\alpha_k}{\sum_{k=1}^{m}\frac{1}{\alpha_k}}. \tag{36}$$

Recognizing $\left(\tilde{v}_m^{p}\right)^2$ in the second term of equation 36, we have

$$\left(\tilde{v}_m^{\alpha\beta}\right)^2 = \gamma\,\left(\tilde{v}_m^{\alpha}\right)^2 = \frac{\tilde{v}_m^{\beta}}{\tilde{v}_m^{\alpha}}\,\left(\tilde{v}_m^{\alpha}\right)^2 = \tilde{v}_m^{\beta}\tilde{v}_m^{\alpha}. \tag{37}$$

Equation 37 is used in the body of this paper to convert P-wave and S-wave estimation of pore pressure to an estimate that is based on PS-wave stacking velocity.

REFERENCES

Dix, C. H., 1955, Seismic velocities from surface measurements: Geophysics, **20**, No. 1, 68–86. URL `http://link.aip.org/link/?GPYSA7/20/68/1`

Eaton, B. A., 1969, Fracture gradient prediction and its application in oilfield operations: Journal of Petroleum Technology, **10**, 1353–1360.

Eaton, B. A., 1972, Graphical method predicts geopressure worldwide: World Oil, **182**, No. 6, 51–56.

Eaton, B. A., 1975, The equation for geopressure prediction from well logs, 1–11.

Ebrom, D., Heppard, P., Mueller, M., and Thomsen, L., 2003, Pore pressure prediction from S - wave, C - wave, and P - wave velocities: SEG, Expanded Abstracts, **22**, No. 1, 1370–1373.

Ebrom, D., Heppard, P., and Thomsen, L., 2002, Numerical modeling of ps moveout as a function of pore pressure: SEG, Expanded Abstracts, **21**, No. 1, 1634–1637.

Kumar, K. M., 2008, Pore pressure using 4-component ps-wave seismic velocities: Ph.D. thesis, University of Texas.

Kumar, K. M., Ferguson, R. J., Ebrom, D., and Heppard, P., 2006, Pore pressure prediction using an Eaton's approach for PS - waves: SEG, Expanded Abstracts, **25**, No. 1, 1550–1554.

Snijder, J., David Dickson, D., Hillier, A., Litvin, A., Gregory, C., and Phil Crookall, P., 2002, 3d pore pressure prediction in the columbus basin, offshore trinidad and tobago: First Break, **20**, 283–286.

Tessmer, G., and Behle, A., 1988, Common reflection point data-stacking technique for converted waves: Geophysical Prospecting, **36**, No. 7, 671–688.